NANO LETTERS

2007
Vol. 7, No. 7
2157−2161

# Nanoscale Additives Tailor Energetic Materials

**David L. Reid, Antonio E. Russo,† Rodolphe V. Carro, Matthew A. Stephens, Alexander R. LePage, Thomas C. Spalding, Eric L. Petersen, and Sudipta Seal***

*Mechanical, Materials and Aerospace Engineering, Advanced Materials Processing and Analysis Center, Nanoscience and Technology Center, University of Central Florida, Orlando, Florida 32816*

*Received October 28, 2006; Revised Manuscript Received December 31, 2006*

**ABSTRACT**

**The effect of anatase, rutile, and amorphous $TiO_2$ nanoparticles on the combustion of solid rocket propellant was investigated. Each additive increased the burning rate of propellant strands by 30%. Typical fast-burning propellants are unstable due to oversensitivity to pressure variations, but the anatase additive yielded propellants with high yet stable burning rates over a broad pressure range. Anatase nanoparticles also catalyzed the high-temperature decomposition of ammonium perchlorate, a key component of solid propellant.**

In 1972, Fujishima and Honda demonstrated the splitting of water on a $TiO_2$ electrode,[1] and in the years since, titania, a material traditionally of note for its use in pigments, has become one of the most intensely studied materials for catalytic applications. Focus has shifted more recently to nanostructured titania, which exhibits remarkable properties due to the combined phenomena of high surface area and quantum size effects.[2] Bulk titania exists in nature primarily in the rutile phase, and thus the structure and reactivity of rutile surfaces have been well-characterized over the past several decades.[3] However, recent interest in the use of nanoscale titania has revealed that anatase often shows superior performance in important applications, including photocatalysis[4] and solar cells.[5] Preparation method also plays an important role, as it influences the particle size, morphology, electronic structure, and surface properties.[6−8]

While much of the current literature concentrates on its photoinduced activity,[4] nanoscale titania is finding use in other novel areas as well. A recent study[9] found that amorphous sol−gel derived $TiO_2$ nanoparticles improved the burning characteristics of solid rocket propellant. In the current study, we explore the effect of nanostructured anatase, rutile, and amorphous titania on the burning of solid propellant. Further, we propose a reaction mechanism by studying the decomposition of ammonium perchlorate (AP), a key component of composite solid propellant, in the presence of titania nanoadditives. While previous studies using traditional (micron) powders found that $TiO_2$ had no effect on AP decomposition,[10] we report the strong catalytic activity of anatase nanoparticles toward this reaction.

The use of powder additives to modify the burning rate of solid propellants and other energetic materials has been the topic of much study for several decades. Oftentimes, applications dictate the need for propellants with tailored burning rates to meet specific and varied goals. In some cases, higher or lower burning rates are desired, while in others a stable burning rate, insensitive to pressure variations, is preferable. The latter is traditionally difficult to achieve over a wide pressure range, and to date, the ability of certain additives to modify the burning rate of propellants had met with mixed success.[11] Nanoscale powder additives such as titania hold promise for heretofore unrealized capability for the tailoring of energetic reactions.

Amorphous titania nanoparticles were prepared by a typical sol−gel method using acetylacetone as a stabilizing agent. Subsequent annealing at 250, 400, and 800 °C produced amorphous, anatase, and rutile powders, respectively. The XRD patterns of the annealed powders are shown in Figure 1. The 800 °C annealed sample contained approximately 12% anatase by mass, as calculated from a comparison of the anatase (101) and rutile (110) integrated XRD peak intensities.[12] The mean particle sizes of the anatase and rutile powders were calculated to be 15 and 50 nm, respectively, from Williamson−Hall plots of the XRD data and Scherrer's formula. TEM images of the anatase and rutile additives are shown in Figure 2, indicating that the dried powders are agglomerates with relatively broad distributions of crystallite size and shape, with average crystallite sizes of approximately 15 and 200 nm for the anatase and rutile powders, respectively. The discrepancy between the actual rutile particle size and that calculated by XRD is due to unaccounted-for instrumental XRD peak broadening. The

* Corresponding author. E-mail: sseal@mail.ucf.edu.
† Visiting Student, NSF-REU Program, Carnegie Mellon University.

10.1021/nl0625372 CCC: $37.00 
**Published on Web 06/12/2007**

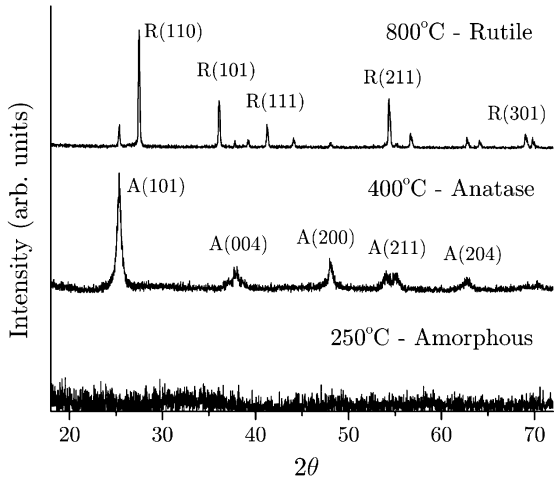


**Figure 1.** XRD patterns of $TiO_2$ nanoparticles annealed at 250, 400, and 800 °C showing amorphous, anatase, and rutile phases, respectively.

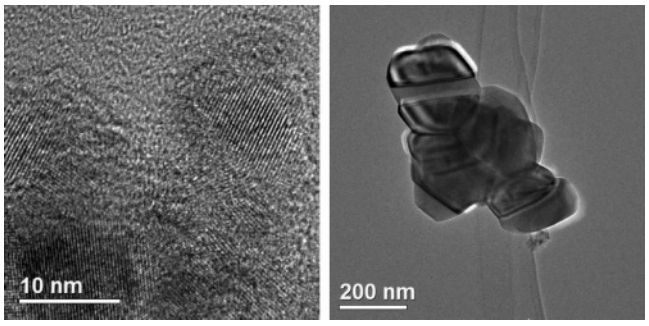


**Figure 2.** TEM images of the anatase (left) and rutile (right) additives.

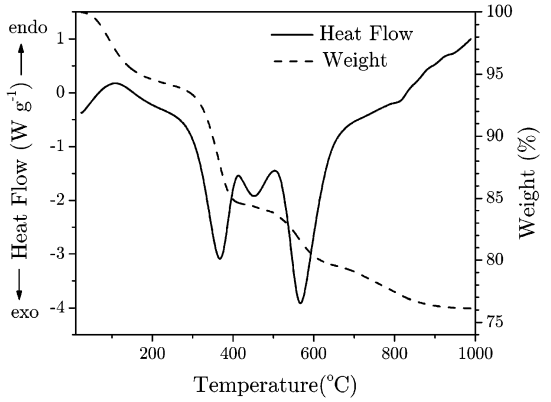


**Figure 3.** DSC and TGA plots of the amorphous $TiO_2$ additive.

BET surface areas of the agglomerated amorphous, anatase, and rutile powders were 29, 35, and 3.5 $m^2\ g^{-1}$, respectively. DSC and TGA plots of the 250 °C-treated powder, conducted at 20 °C $min^{-1}$ under flow of air, are shown in Figure 3. The endothermic peak centered around 100 °C corresponds to the removal of water with a weight loss of 5.9%. The two large exothermic peaks at 370 and 570 °C are attributed to the decomposition and combustion of organic residues, with corresponding weight losses of 9.4% and 5.1%, respectively. The smaller exothermic peak at 452 °C is attributed to the amorphous-to-anatase phase transformation, while the anatase-to-rutile transformation may be indicated by the small hump at 815 °C. The total weight loss for the sample was 23.8%. The 400 °C annealed powder underwent a continuous weight loss of 1.9% up to 1000 °C, and the 800 °C annealed powder exhibited no measurable weight loss.

The effect of each $TiO_2$ additive on the thermal decomposition of AP was studied by DSC/TGA analysis, carried out at 10 °C $min^{-1}$ in open sample pans under a flow of argon. Samples of pure AP and AP mixed with each additive on a 1% by mass basis were prepared by grinding the powders with a mortar and pestle until homogeneous. While the amorphous additive contained only 76% $TiO_2$ by mass, this was not seen to significantly affect the experimental results. The thermal decomposition of AP takes place in three steps, as described by Boldyrev:[13] The first is an endothermic phase transition from orthorhombic to cubic at 240 °C with no associated weight loss. At 270 °C, there is an exothermic process referred to as the low-temperature decomposition (LTD). The LTD is a heterogeneous process beginning with proton transfer in the AP subsurface, yielding $NH_3$ and $HClO_4$ adsorbed in the porous structure that forms during the reaction, followed by the decomposition of $HClO_4$ and reaction with $NH_3$. As the LTD proceeds, the pores become saturated with adsorbed $H_2O$ (a product of the decomposition), and the reaction ceases after approximately 30% weight loss. At 350 °C, the high-temperature decomposition (HTD) begins on the AP surface and proceeds until completion at 455 °C. The HTD involves the simultaneous dissociation and sublimation of AP to $HClO_{4(g)}$ and $NH_{4(g)}$. It has been observed[14] that the HTD is endothermic if the decomposition takes place at atmospheric pressure and under a flow of inert gas or air; however, at higher pressures or under conditions in which the evolved gases remain in close contact (such as in closed sample pans), the reaction is exothermic due to the oxidation of ammonia by the acid in the gas phase. Jacobs and Whitehead[10] summarized the AP decomposition reactions, as shown in eq 1. While the actual process involves many additional steps (and is not yet fully understood), the preceding mechanistic description is useful for interpreting the effect of additives.

$$\begin{array}{ccccc} NH_4^+ + ClO_4^- & \rightleftharpoons & NH_{3(a)} + HClO_{4(a)} & \longrightarrow & \text{LTD products} \\ \Updownarrow & & \Updownarrow & \textit{sublimation} & \\ \text{sublimate} & \longleftarrow & NH_{3(g)} + HClO_{4(g)} & \longrightarrow & \text{HTD products} \end{array} \quad (1)$$

Representative DSC curves for the decomposition of AP mixed with 1% by mass of each additive are shown in Figure 4, and Table 1 shows a summary of the important peaks and transitions from the DSC/TGA analysis. The additives did not affect the AP phase transformation. The effect on the LTD was similar for each additive. The LTD enthalpy was increased from −28.1 kJ $mol^{-1}$ for pure AP to −17.5, −17.9, and −18.0 kJ $mol^{-1}$ for the amorphous, anatase, and rutile additives, respectively, and LTD onset temperature was reduced by about 1 °C. A significant difference between the additives was observed in their effect on the HTD. The HTD enthalpy for pure AP was +54 kJ $mol^{-1}$. With the amorphous

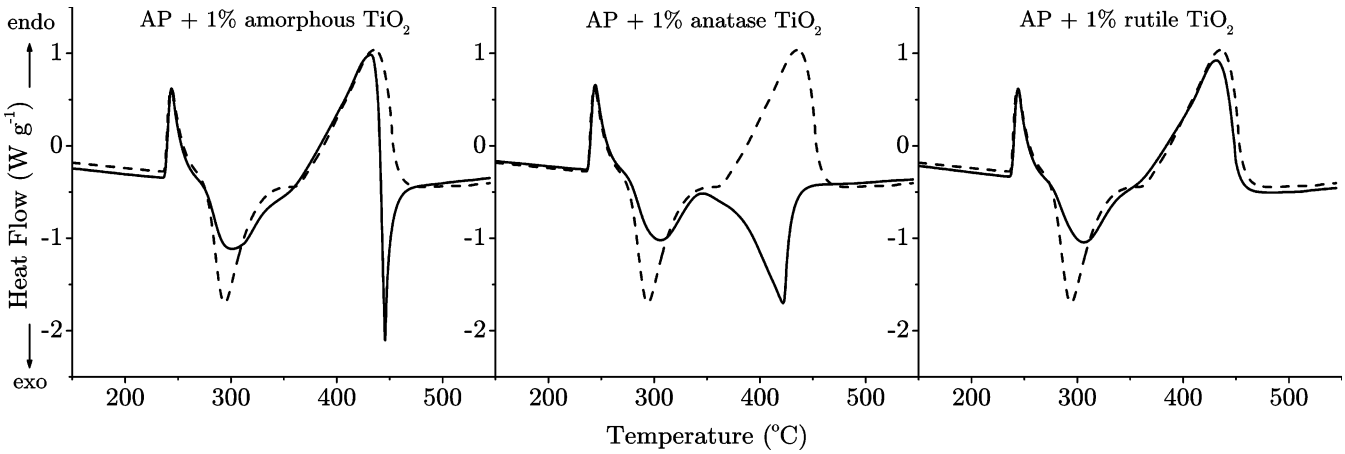


**Figure 4.** DSC curves for the decomposition of AP with 1% amorphous, anatase, and rutile titania additives. In each plot, the decomposition of pure AP is shown by the dashed line.

**Table 1.** DSC/TGA Summary of the Decomposition of AP with and without 1% Amorphous, Anatase, and Rutile Titania Additives[a]

| additive | LTD onset °C | LTD enthalpy kJ mol$^{-1}$ | LTD wt loss % | HTD onset °C | HTD enthalpy kJ mol$^{-1}$ | HTD wt loss % | end temp °C |
|---|---|---|---|---|---|---|---|
| pure AP | 277.1 ± 0.2 | −28.1 ± 0.6 | 26.3 ± 0.6 | 361.2 ± 0.9 | +54 ± 2 | 73.2 ± 0.5 | 453 ± 2 |
| 1% amorphous | 275.8 ± 0.2 | −17.5 ± 0.7 | 19.6 ± 0.8 | 347.7 ± 0.7 | +48 ± 9 | 79.3 ± 0.9 | 447 ± 2 |
| 1% anatase | 275.9 ± 0.3 | −17.9 ± 0.3 | 19.9 ± 0.2 | 345.7 ± 0.0 | −27 ± 5 | 79.0 ± 0.7 | 423 ± 2 |
| 1% rutile | 275.3 ± 0.0 | −18.0 ± 0.8 | 18.4 ± 0.4 | 350.2 ± 2.1 | +56 ± 6 | 80.5 ± 0.1 | 449 ± 1 |

[a] Results are the average of triplicate experiments.

additive, a sharp exothermic peak appeared at the very end of the decomposition, and the overall enthalpy for the HTD transition (endothermic + exothermic peaks) was +48 kJ mol$^{-1}$. With anatase, the HTD peak was completely exothermic, with an enthalpy of −27 kJ mol$^{-1}$. The rutile additive had little effect on the HTD, with an enthalpy of +56 kJ mol$^{-1}$. The two phases of AP decomposition are distinguishable in the TGA weight curves shown in Figure 5. The LTD weight loss occurs from about 275−350 °C; the remaining weight loss is attributed to the HTD step. For pure AP, the weight loss during the LTD and HTD were 26.3% and 73.2%, respectively (about 0.5% remains as solid residue). The amorphous, anatase, and rutile additives

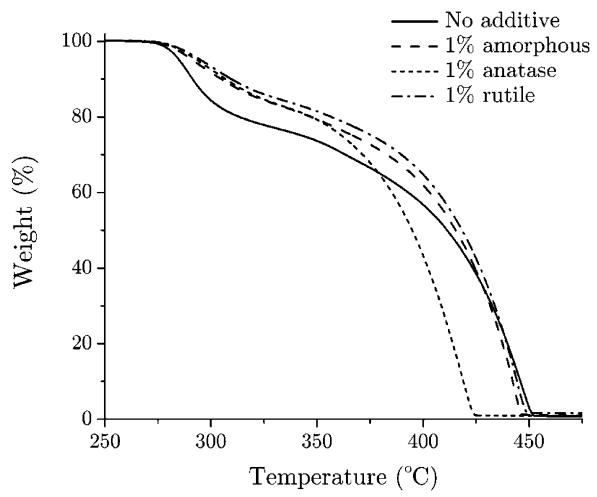


**Figure 5.** TGA plots of the decomposition of AP with 1% amorphous, anatase, and rutile titania additives.

reduced the LTD weight loss by roughly equal amounts to 19.6%, 19.9%, and 18.4%, respectively. The amorphous and rutile additives had little effect on the HTD weight loss profile, while anatase accelerated the HTD and reduced the completion temperature from 453 °C for pure AP to 423 °C with the additive.

The DSC/TGA results show that each titania additive inhibits the LTD, although the mechanism for this is not clear. It is unlikely that $TiO_2$ particles would affect solid-state decomposition reactions. The effect may result from a reduction in AP particle size when it was ground together with the additives during sample preparation. The BET surface area of AP mixed with 1% $TiO_2$ roughly doubled (from 3 to 6 m$^2$ g$^{-1}$ for the case of the anatase additive) when AP and the additive were ground together, as opposed to separately. Lang and Vyazovkin[14] found that reducing the particle size of AP by milling lowered the LTD peak intensity but had little effect on the HTD, supporting this explanation. In terms of potential applications, the HTD is of primary interest because it occurs at temperatures similar to the surface temperature of burning solid propellant. During the HTD decomposition of pure AP, the products $NH_3$ and $HClO_4$ are carried away in the purge gas stream and the decomposition is completely endothermic. The exothermic nature of the HTD in the presence of anatase can be attributed to the adsorption and catalytic oxidation/reduction of the gaseous products on the titania nanoparticle surfaces; thus a combination of the typical endothermic decomposition plus an exothermic surface reaction of greater magnitude results in an overall exothermic peak. Ammonia is known to adsorb molecularly on $TiO_2$ surfaces at the fivefold coordinated Ti

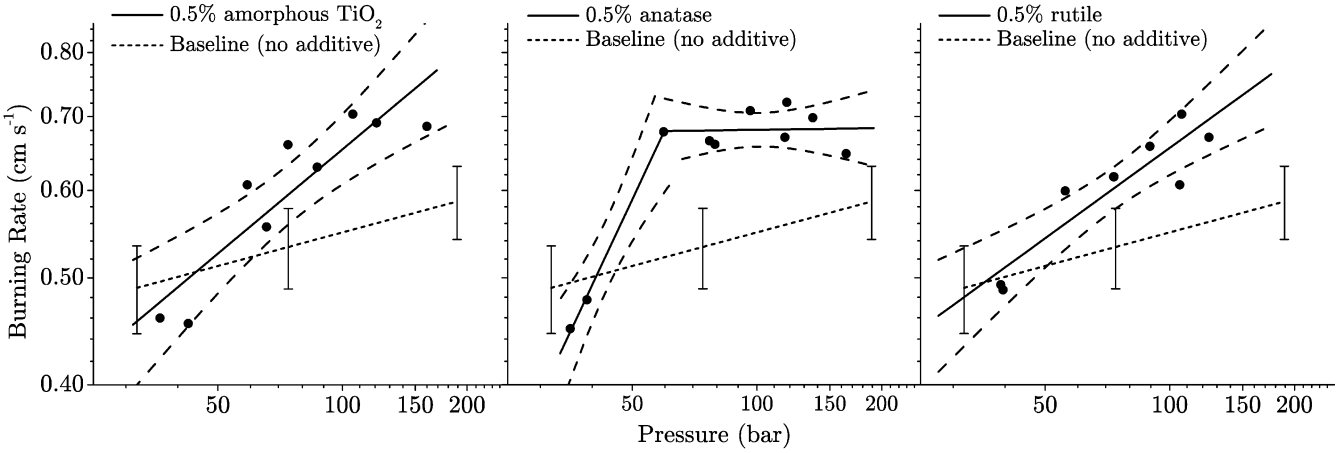


**Figure 6.** Linearized plots of solid propellant burning rates vs pressure on a log−log scale. Solid lines indicate the burning rates with titania additives; the surrounding dashed lines indicate the 95% confidence intervals for the linear fits. Short-dashed lines indicate a baseline generated from repeated experiments on propellants with a standard (no additive) composition, and error bars of ± one standard deviation.

sites,[3] and $TiO_2$ has been shown to catalyze the decomposition of $HClO_4$ in the temperature range 300−1000 °C.[15] The 15 nm anatase nanoparticles produced for the current study have a far greater specific surface area than the 200 nm rutile particles, and thus it is expected that anatase would be the more efficient catalyst. However, surface area differences alone cannot account for the total lack of a similar HTD catalytic effect with rutile and amorphous additives, and a different mechanism may be at work. The amorphous additive undergoes a phase transition to anatase around 450 °C. Assuming that only anatase catalyzes the HTD, the transformation to anatase could explain the exothermic peak observed at the very end of the HTD with the amorphous additive. However, due to the sharpness of the peak, it is more likely to result from the thermal explosion of the remaining AP, which is known to occur spontaneously at temperatures above 440 °C.[16] The amorphous additive, being approximately 18% organic residue by mass, still consists of 8% organics after heating to 440 °C, providing a fuel for the explosion that is not present in the other additives.

Given the enhanced activity of anatase toward AP decomposition, one could expect that it would also enhance the burning rate of solid rocket propellant. The components of a typical solid propellant include aluminum powder as fuel, AP as oxidizer, and a polymer binder such as hydroxy-terminated polybutadiene, which is also a secondary fuel. AP undergoes a thermal decomposition to ammonia and perchloric acid when the propellant ignites, providing the source of active oxygen for the energetic reaction of aluminum to aluminum oxide. A nonmetallized propellant formulation was used in the current study to provide a more simple system to isolate the additive effects. Propellants containing 70% AP, 0.5% additive by mass, and the remainder HTPB binder and curative, were mixed and extruded by hand to form cylindrical strands 25 mm in length. Propellant burning rates were measured in a strand bomb reactor following the procedure reported by Carro et al.[17]

According to Vieille's Law,[18] propellant burning rates increase exponentially with pressure, as shown in eq 2:

$$r = ap^n \qquad (2)$$

where the pre-exponential factor $a$ and the pressure exponent $n$ are constants for a given propellant. Pressure and light emission were recorded during each propellant burn, and the burning rate $r$ was calculated as the duration of the burn divided by the length of the propellant strand. The pressure $p$ was taken as the average pressure throughout the burn. Figure 6 shows the linearized burning rate curves for propellants with each additive, as calculated from eight to ten propellant strands burned throughout the pressure range. These results were duplicated with a second batch of additives and propellants (see Supporting Information). The baseline for propellants containing no additive was calculated from previous experiments conducted by our group.[19] All three additives increased the burning rates relative to the baseline, and the propellants containing anatase exhibited two distinct regions: from 30−60 bar, the burning rates increased exponentially with pressure, but from 60−200 bar, the burning rate was constant. The calculated values of $a$ (in units of cm $s^{-1}$) and $n$ were 0.63 and 0.10 for the baseline, 0.44 and 0.31 for amorphous $TiO_2$, 0.48 and 0.27 for rutile, 0.20 and 0.80 for the anatase pre-plateau region, and 0.83 and 0.0052 for the anatase plateau, respectively. These results correspond to a maximum burning rate increase of approximately 30% for each additive.

A burning rate plateau is a desirable feature for high-burning-rate propellants. Typical propellant formulations that achieve a high burning rate by increasing the value of the pressure exponent are unstable due to their oversensitivity to pressure variations, which can lead to catastrophic failure. The anatase additive provides a propellant with a burning rate that is both high and stable over an extended pressure range. The plateau observed with the anatase additive may indicate that a surface reaction becomes the rate-limiting step at pressures above 60 bar, while at lower pressures, the reaction is diffusion-limited. This simplified mechanism agrees with the DSC/TGA results showing the catalytic oxidation/reduction of gaseous AP decomposition products on the anatase nanoparticles. However, amorphous and rutile additives also increased the propellant burning rates but did not catalyze AP decomposition. Other mechanisms are

certainly involved in the complex reactions of solid propellant combustion.

Our results emphasize that, through control over structure, the properties of nanoscale titania can be made favorable for new and promising applications. The anatase structure showed enhanced activity over rutile or amorphous $TiO_2$ for the catalysis of energetic reactions. Further work may lead to additives for safer and more efficient solid rocket propulsion or the ability to meet application-specific propellant requirements through the tailoring of additive structure on the nanoscale.

**Acknowledgment.** We thank the National Science Foundation (EEC 0453436) and the Missile Defense Agency for funding to support this work, and Sameer Deshpande for the TEM images. Approved for Public Release, 06-MDA-2061 (29 May 2007).

**Supporting Information Available:** Methods and supporting data. This material is available free of charge via the Internet at http://pubs.acs.org.

## References

(1) Fujishima, A.; Honda, K. *Nature* **1972**, *238*, 37.
(2) Abrams, B. L.; Wilcoxon, J. P. *Crit. Rev. Solid State Mater. Sci.* **2005**, *30*, 153.
(3) Diebold, U. *Surf. Sci. Rep.* **2003**, *48*, 53.
(4) Carp, O.; Huisman, C. L.; Reller, A. *Prog. Solid State Chem.* **2004**, *32*, 33.
(5) Barbé, C.; Arendse, F.; Comte, P.; Jirousek, M.; Lenzmann, F.; Shklover, V.; Grätzel, M. *J. Am. Ceram. Soc.* **1997**, *80*, 3157.
(6) Barnard, A. S.; Curtiss, L. A. *Nano Lett.* **2005**, *5*, 1261.
(7) Allen, N. S.; Edge, M.; Ortega, A.; Liauw, C. M. *Dyes Pigm.* **2006**, *70*, 192.
(8) Li, Y.; White, T. J.; Lim, S. H. *J. Solid State Chem.* **2004**, *177*, 1372.
(9) Small, J.; Stephens, M.; Deshpande, S.; Petersen, E.; Seal, S. In *20th International Colloquium on the Dynamics of Explosions and Reactive Systems*; McGill University: Montreal, Canada, 2005.
(10) Jacobs, P. W. M.; Whitehead, H. M. *Chem. Rev.* **1969**, *69*, 551.
(11) Brill, T.; Budenz, B. *Solid Propellant Chemistry, Combustion, and Motor Interior Ballistics*; AIAA: Reston, VA, 2000; pp 3−32.
(12) Zhang, H.; Finnegan, M.; Banfield, J. *Nano Lett.* **2001**, *1*, 81.
(13) Boldyrev, V. *Thermochim. Acta* **2006**, *443*, 1.
(14) Lang, A. J.; Vyazovkin, S. *Combust. Flame* **2006**, *145*, 779.
(15) Solymosi, F.; Gera, L.; Börcsök, B. *Kinet. Katal.* **1976**, *8*, 299.
(16) Galwey, A. K.; Jacobs, P. W. M. *J. Chem. Soc.* **1960**, 5031.
(17) Carro, R.; Arvanetes, J.; Powell, A.; Stephens, M. A.; Petersen, E. L.; Smith, C. *AIAA Paper 2005−3617*, 2005.
(18) Sutton, G. P.; Biblarz, O. *Rocket Propulsion Elements*; Wiley & Sons: New York, 2001.
(19) Stephens, M.; Sammet, T.; Carro, R.; LePage, A.; Reid, D.; Seal, S.; Petersen, E. *AIAA Paper 2006−4948*, 2006.

NL0625372